Post Monsoon Season Spatial Distribution of Groundwater Depth over the Low-Lands of Sunsari District of Eastern Nepal

D. Ghimire, D. R. Dhakal, G. Bhusal, A. K. Khadka, S. Shrestha and R. P. Regmi

Journal of Nepal Physical Society

Volume 8, Issue 3, December 2022

ISSN: 2392-473X (Print), 2738-9537 (Online)

JNPS, **8** (3): 32-38 (2022)

DOI: https://doi.org/10.3126/jnphyssoc.v8i3.50723

Published by:

Nepal Physical Society
P.O. Box: 2934
Tri-Chandra Campus
Kathmandu, Nepal
Email: nps.editor@gmail.com

JNPS 8 (3): 32-38 (2022)
ISSN: 2392-473X (Print), 2738-9537 (Online)
Research Article *© Nepal Physical Society*
DOI: https://doi.org/10.3126/jnphyssoc.v8i3.50723

Post Monsoon Season Spatial Distribution of Groundwater Depth over the Low-Lands of Sunsari District of Eastern Nepal

D. Ghimire*, D. R. Dhakal, G. Bhusal, A. K. Khadka, S. Shrestha and R. P. Regmi
National Atmospheric Resource and Environmental Research Laboratory,
Central Department of Physics, Tribhuvan University, Kirtipur, Kathmandu, Nepal
*Corresponding Email: dhirug2@gmail.com

Received: *1st July, 2022;* ***Revised:*** *22nd Oct., 2022;* ***Accepted:*** *3rd Dec., 2022*

ABSTRACT

The knowledge and an accurate representation of the spatial distribution of groundwater depth of an area are very important to realize sustainable use of groundwater resource, protection of ecosystem and for the development of adaptation policies in the changing climate. The present study has, thus, developed a groundwater depth distribution map of southern low-lands of the Sunsari District at the horizontal grid resolution of 3 km × 3 km. The groundwater depths were surveyed at predefined 82 numbers of geo-referenced grid points scattered over the region during the post monsoon season of the year 2019. Referencing the sampled depths, spatial distribution of the groundwater depth over the area has been predicted using the Ordinary Kriging Method. Three widely used Semivariogram modules such as Spherical, Exponential, and Gaussian were implemented. The Gaussian model of Semivariogram outperformed the other methods with R^2 of 0.336, *RMSE* of 2.591, and *MAE* of 1.946. The predicted spatial distribution of groundwater depth reasonably well correlated with the observed distribution. The spatial distribution of groundwater level suggests that 12.36% the total area, particularly, over the western, southwestern and northern parts hold groundwater at much shallower depth (< 5 m). Over 51.59 % of the total area in the southeastern and northeastern parts, the groundwater level remained below 8 m from the ground and the rest of the total area holds the groundwater deeper than 8 m.

Keywords: Spatial Distribution, Groundwater, Interpolation, Kriging, Semivariogram.

1. INTRODUCTION

Adequate information on spatial variation of groundwater depths is prerequisite to the proper planning, risk assessment and decision making for the sustainable development of groundwater resources. A regional scale assessment of groundwater distribution with the conventional method of direct measurements to generate densely populated data may not be viable as they are inherently expensive and time consuming [1].

However, recent advancement in the numerical interpolation techniques has made it possible to realize a realistic assessment of groundwater distribution at desired spatial resolution with sparsely available observation data. Several studies [e.g., 2, 3, and 4] have demonstrated efficient and reasonably accurate assessments of regional scale spatial distribution of groundwater depth using the limited number of observed data from the area. Geographic Information System (GIS) is among the widely used computer-built tools to estimate and map the groundwater surface over an area of interest [5]. The numerical interpolation techniques that it incorporates are considered highly efficient and fairly accurate. Furthermore, the Geostatistical analysis module in GIS is the reliable way to reveal the spatial correlation [6] and is used extensively for incorporating and analyzing spatial data. This particular module of GIS can greatly help simplify arrangement of resource expansion, ecological safety and logical investigation [7]. In recent years, the use of GIS has grown rapidly in various studies related to groundwater assessment and development.

For mapping of groundwater depth, the most traditional and routinely used interpolation techniques includes deterministic and stochastic approach. Kriging, a set of methods, completely based on the statistical properties of the sample data points is the most commonly used stochastic approach of interpolation. Derived from the name, D. G. Krige, one who introduced the use of moving averages to avoid systematic errors in interpolation, is known as the best linear unbiased estimate [8]. Numerous papers have been published related to the applicability of Kriging Interpolation methods [6, 9, 10, 2, 11, and 12]. Ordinary Kriging is most commonly used as a interpolation technique to assess the groundwater status in various areas [4, 9, 10, 11, 12]. Theodossiou and Latinopoulous studied the spatial variability of ground water level in a peninsula of northern Greece to evaluate and optimize ground water observation networks by using OK [9]. Varouchakis and Hristopulos in their research article compared OK with the other interpolation techniques in Greece and found that OK is better than the other counterparts used in the study [4]. Ahmadi and Sedghmiz [10] adopted the OK analysis to reveal the spatial and temporal structure of groundwater level fluctuation. They carried out the spatial and temporal analysis of monthly groundwater level fluctuations of 39 peizometric wells in Darab plain of southern Iran that was monitored for 12 years and found that there exists a strong spatial and temporal structure for groundwater level fluctuations. Nikroo et al. (2010) conducted the OK analysis of the non-uniformly spaced observation in Iran and found a strong spatial relationship between the water table elevations of the wells [11]. Dash et al. compared the Kriging interpolators and showed that OK is a useful tool to elucidate those areas lacking enough data for developing a water table management network [12].

Although, no prior studies on the regional scale distribution of groundwater level using the Kriging Interpolation techniques are available, studies around the world in diverse landscapes as discussed above suggest that the same method can be expected to provide a realistic estimation of groundwater distribution over the low land areas of Sunsari District of Eastern Nepal at local scale. To our best knowledge, Ordinary Kriging interpolation technique has not been used in Nepal for groundwater distribution mapping. However, several GIS tools have been used extensively for studying the groundwater quality [13] and groundwater exploitation [14] in different regions in Nepal. Thus, present study is conceived to understand the spatial distribution of groundwater surfaces over the low-lands of Sunsari District of Eastern Nepal. The study is expected to address the research gap in the field of groundwater spatial distribution in the study area and thus provide the adequate information for the scientific management of groundwater resources for its sustainable development.

2. MATERIALS AND METHODS

2.1 Study area and data collection

The study area is the low-land region of the Sunsari District of Eastern Nepal (Fig. 1). The district lies between 26^0 $24^{'}$ $6^{"}$ N to 26^0 $52^{'}$ $52^{"}$ N and 86^0 $54^{'}$ $12^{"}$ E to 87^0 $21^{'}$ $13^{"}$ E, with a total area of 1275 km^2. However, the present study covers the area of about 820 km^2 which is about 65% of the total area of the Sunsari District. The area is characterized by the subtropical monsoon climate. Summers are hot and wet and winters are mild and dry. Average air surface temperature ranges from a minimum of about 9^0 C in winter to the maximum of about 40^0 C in summer. The mean annual precipitation in the Sunsari district is 1794.30 mm and 85% of the rainfall occurs during June to September.

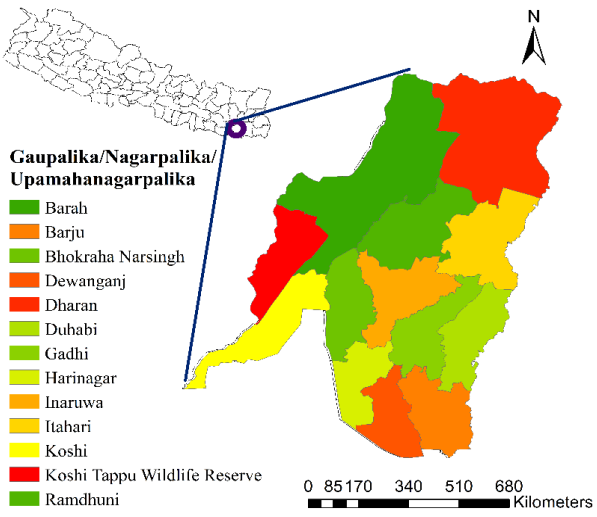

Fig. 1: The location and geographic coverage of the Sunsari district in the map of Nepal as prepared using the ArcGIS 10.7.1.

To gather the water table data, the field survey was conducted. This data was collected in the post monsoon season of year 2019. The survey was done in the 82 locations at the horizontal grid resolution

of 3 km × 3 km and the coordinates of the locations were identified with the help of Global Positioning System (GPS). This data was input for the interpolation and estimation of groundwater surface distribution over the low-lands of Sunsari District.

2.2 Ordinary Kriging

In this method, the mean of the variable value in observation points, *m*, is assumed to be unknown. $Z^*(x_0)$, the interpolated variable at location x_0 is determined by using the equation:

$$Z^*(x_0) = \sum \lambda_i Z(x_i) \quad \text{.....(1)}$$

where, *n* is the number of observation points, x_i is the location of the i^{th} observation, λ_i is the weight chosen for x_i so as to satisfy unbiasedness and minimum variance, and $Z(x_i)$ is the value of variable at i^{th} observation point.

Semivariogram analysis aids the Kriging interpolators such as Ordinary Kriging to quantify the spatial dependence of measured sample [3]. It is a diagram in which half of the variance of the difference between the variables with distance *h* from each other i.e., $\gamma(h)$ is plotted against *h*. The $\gamma(h)$ is calculated as,

$$\gamma(h) = \frac{1}{2n(h)} \sum_i^{n(h)} [Z(x+h) - Z(x)]^2 \quad \text{.....(2)}$$

Where $n(h)$ denotes the number of pairs of samples used in the calculation for each distance *h*, *Z(x)* is the observed variable, and $Z(x+h)$ is the observed variable situated in the distance *h* from *Z(x)* [15]. Theoretically, at $h = 0$, the value of $\gamma(h)$ is zero. But empirically, it has been found that, even at $h = 0$, Semivariogram has a small value called nugget as shown in Figure 3 [11, 16]. Then, with an increase in *h*, $\gamma(h)$ also increases till it approaches a constant value called sill. The value of *h* at which $\gamma(h)$ approaches a constant value is called range. Spatial dependence of the variables (groundwater depth in our case) is directly reflected by the nugget effect and the nugget to sill ratio [17]. A variable is said to have strong spatial dependence if the nugget to sill ratio is less than 0.25, and has a moderate spatial dependence if the ratio is in between 0.25 and 0.75; otherwise, the variable has a weak spatial dependence [3]. Based on the pattern of plotted points, different kinds of functions can be fitted to the Semivariogram. The most common functions for modeling the Semivariogram are Spherical, Exponential and Gaussian models. These models are determined by the following equations [11, 18, 19, 20].

Spherical model of Semivariogram:

$$\gamma(h) = C\left[\left(\frac{3h}{2a}\right) - \left(\frac{h^3}{2a^3}\right)\right] + C_0 \; ; h \le a$$
$$= C + C_0 \; ; h > a \quad \text{.....(3)}$$

Exponential model of Semivariogram:

$$\gamma(h) = C\left[1 - exp\left(-\frac{h}{2a}\right)\right] + C_0 \; ; h \le a$$
$$= C + C_0 \; ; h > a \quad \text{.....(4)}$$

Gaussian model of Semivariogram:

$$\gamma(\mathrm{h}) = \mathrm{C}\left[1 - \exp\left(-\frac{\mathrm{h}^2}{\mathrm{a}^2}\right)\right] + \mathrm{C}_0 \; ; \; \forall \mathrm{h} \quad \text{.....(5)}$$

These models were adjusted to the experimental Semivariogram by the Geostatistical Analyst tool of GIS, and the following parameters were defined; nugget (C_0), sill ($C_0 + C$) with *C* as the partial sill and range (a). As soon as the best fit model for the interpolation method were determined, the parameters of the best fit model (Nugget, Sill and Range) were calculated.

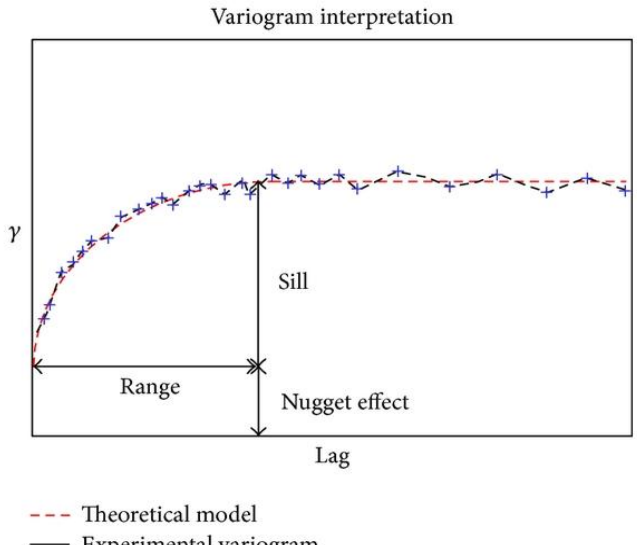

Fig. 2: Semivariogram model [16].

To identify the best-fit Semivariogram model, the cross-validation process was employed. Interpolated maps were created using each of the spherical, exponential, and Gaussian models of Semivariogram and were compared to find the Semivariogram model yielding the best results. In the present study, the most commonly used statistical parameters (coefficient of determination (R^2), root mean square error (RMSE), and mean absolute error (MAE)) were used to evaluate the interpolation techniques [2, 3, 21, and 22].

$$R^2 = \left(\frac{\sum Z_i Z - \frac{\sum Z_i \sum Z}{n}}{\sqrt{\left[\sum {Z_i}^2 - \frac{(\sum Z_i)^2}{n}\right]\left[\sum Z^2 - \frac{(\sum Z)^2}{n}\right]}} \right)^2 \quad \text{.....(6)}$$

$$RMSE = \sqrt{\frac{\sum (Z_i - Z)^2}{n}} \quad \text{.....(7)}$$

$$MAE = \frac{1}{n} \sum |Z_i - Z| \quad \text{.....(8)}$$

Where, $Z_i$is the predicted value, Z is the observed value, and n is the number of observations. The Semivariogram model yielding the highest R^2 and the lowest MAE, RMSE is selected as the best-fit model.

3. RESULTS AND DISCUSSIONS

3.1 Spatial distribution of groundwater level

Figure 3a represents the location map of 82 samples together. The general trend of the surveyed groundwater level is shown in Figure 3b. In the figure, X and Y represent the spatial location and Z represents the depth to the groundwater from the surface. Figure 3b illustrates that the depth to groundwater surface increases, in non-linear fashion, as we move from west to east and decreases linearly while moving from south to north. In the figure, blue line represents the trend of the groundwater depth as we move towards north of the study area and green curve represents the trend of depth as we move towards east of the study area.

Descriptive statistics for ground water level measurements are provided in Table 1. Stochastic methods are usually reliable when the data exhibit a normal distribution. Thus, the data were checked for the normal distribution prior to the Ordinary Kriging interpolation by the use of Kolmogorov – Smirnov test (K-S test). K-S test revealed the normal distribution of the groundwater data set.

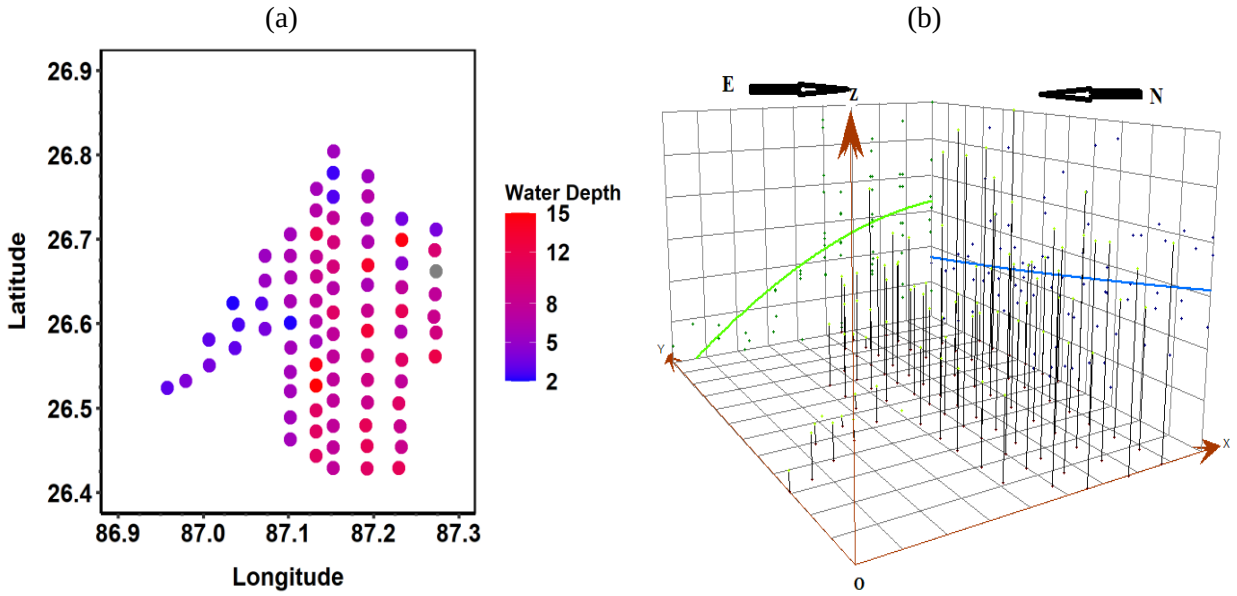

Fig. 3: (a) Location map of 82 groundwater level sample sites colored with depth level and (b) Trend analysis of groundwater level; OZ represents the depth of ground water from the surface.

Table 1: Descriptive statistics of groundwater depth dataset.

Sample size, n	Minimum (m)	Maximum (m)	Mean (m)	Standard Deviation (m)	Skewness	Kurtosis
82	2.1336	15.748	7.6066	3.1997	0.43502	-0.1693

3.2 Spatial structure of groundwater depth

The groundwater depths are interpolated by using Ordinary Kriging method. Three different predefined theoretical Semivariogram models were fitted to the datasets. With maximum R^2 (0.336), and the lowest RMSE (2.591) and MAE (1.946),

Gaussian model of the Semivariogram was found to be the best-fit model for OK method. The parameters of the best-fit Gaussian model are given in the Table 2. Nugget value was 6.852 and sill value was 14.403. Nugget to sill ratio was thus approximately 0.47 which shows that the groundwater depth has a moderate spatial dependence. Thus, in this study, OK method shows that the water table depths were moderately spatially correlated. The range was found as 34.808 km from which it can be inferred that the pair of points that are this distance or greater apart are not spatially correlated. The Semivariogram modeling of the best-fit Gaussian model is presented in Figure 3.

Table 2: Comparison of Semivariogram parameters of OK method for the selection of best-fitted theoretical model

Semivariogram parameters	Nugget, C_0	Sill, C	Range, a (km)	Nugget / Sill	R^2	*RMSE*	*MAE*
Spherical	5.381	13.447	34.808	0.400	0.313	2.639	1.984
Exponential	4.671	7.596	6.708	0.608	0.309	2.650	1.965
Gaussian	6.852	14.403	34.808	0.476	0.336	2.591	1.946

R^2 Coefficient of determination; $RMSE$ root mean square error; MAE mean absolute error

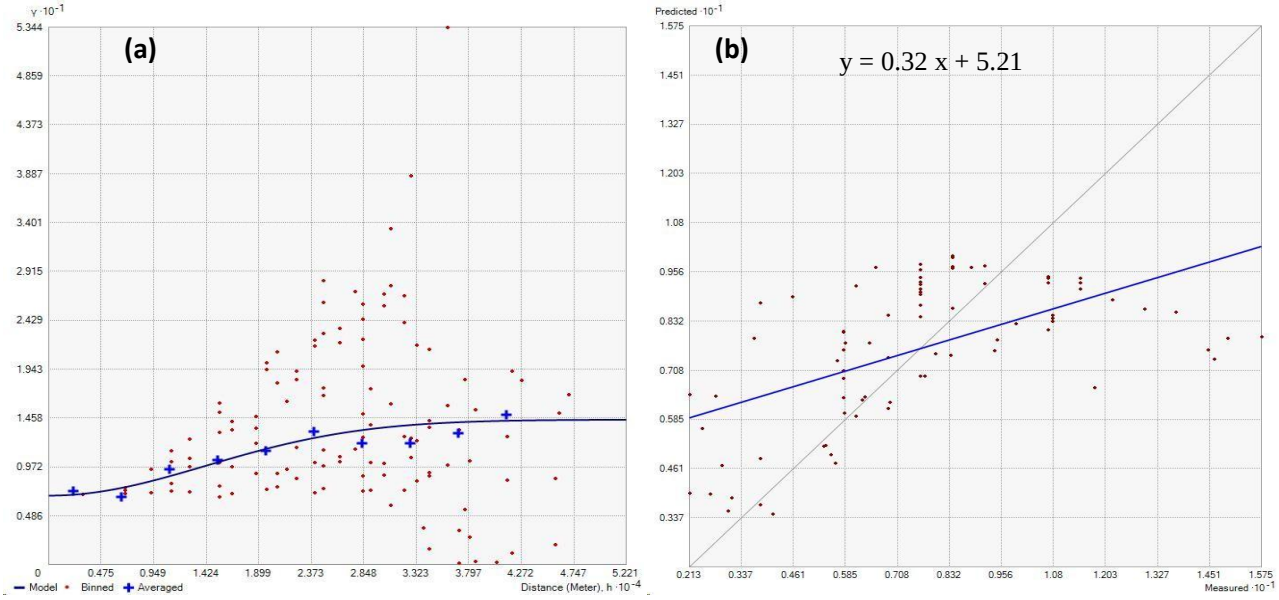

Fig. 4: The best-fit Gaussian model of Semivariogram (a) and Scatter plot of the observed versus predicted groundwater depth (b). The grey line in the right figure represents the 1:1 line and the blue line represents the fitted line (equation is given in the figure).

The scatter plot of predicted values versus the observed values of groundwater depth is shown in Figure 4. Some of the points were lying below the 1:1 line and others above it from which it can be inferred that the Ordinary Kriging method underestimated the larger values and overestimated the smaller values of water table depths.

3.2.1 Spatial distribution of predicted groundwater level

As the OK method with Gaussian model of Semivariogram has given the best prediction, the predicted groundwater depths were visualized from the interpolated surface map using this method.

The interpolated map (figure 5) indicated that comparatively greater depths (> 8 m) were predicted in central, eastern, northeastern and southeastern parts of the study area and the shallower depths (<5 m) were predicted in southwestern, western and northern parts of the low-elevated regions of the Sunsari district.

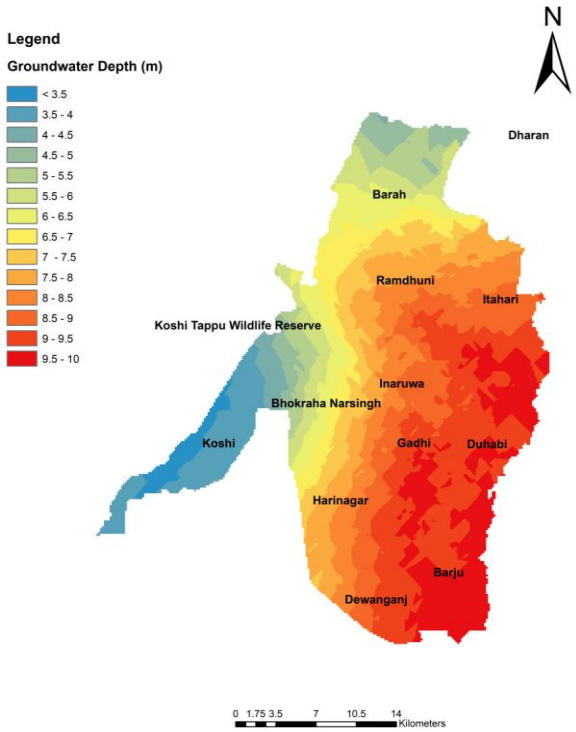

Fig. 5: Predicted spatial distribution of groundwater depth over the low-lands areas of Sunsari District.

Table 3 depicts the area wise distribution of the various groundwater depth ranges. About 12.36 % area is mainly concentrated in the southwestern and northern parts of the study region having water table depth less than 5 m. This might be due to the proximity of Saptakoshi river basin such that the groundwater recharge is very high beneath the surface.

Table 3: Predicted areas of groundwater depth distributions

Groundwater depth (m)	Area (%)
< 3.5	1.86
3.5 – 4	5.83
4 – 4.5	1.51
4.5 – 5	3.16
5 – 5.5	4.05
5.5 – 6	4.78
6 – 6.5	5.91
6.5 – 7	5.87
7 – 7.5	6.29
7.5 – 8	9.15
8 – 8.5	8.91
8.5 – 9	11.04
9 – 9.5	18.62
9.5 – 10	13.02

4. CONCLUSION

Based on the Arc GIS Geostatistical module to analyze the spatial variability of the groundwater depth, this paper compares the simulation accuracies and prediction effects of Ordinary Kriging method aided with three Semivariogram modules: spherical, exponential, and Gaussian models. Gaussian model of Semivariogram was found to be significantly superior to other in the OK interpolation method. Groundwater depths were found to have moderate spatial dependence in the low-lying regions of Sunsari district as indicated by the Nugget/Sill ratio of the optimal model. Major cities like Itahari, Inaruwa, and Duhabi are assessed to have faced severe scarce to the groundwater (groundwater depth >8 m) even during the post monsoon season when the groundwater level is expected to be at much higher compared to the dry season. However, the places nearby the Saptakoshi lying to the southwestern part of the study region have comparatively easier access to the groundwater. Though the scenario of groundwater accessibility in remaining areas as in Central, Northern and Southern are moderate (>5 km and <8 km), it might face unprecedented risk in the near future if the proper groundwater management and control system are not implemented.

5. ACKNOWLEDGEMENT

We are especially indebted to all the local respondents of Sunsari District who shared their time and knowledge for patiently explaining their understanding of groundwater depths distribution during the survey.

REFERENCES

[1] Buchanan, S. and Triantafilis, J. Mapping Water Table Depth Using Geophysical and Environmental Variables. *Ground water*, **47**: 80-96 (2008).

[2] Sun, Y.; Kang, S.; Li, F. and Zhang, L. Comparison of Interpolation Methods for Depth to Groundwater and Its Temporal and Spatial Variations in the Minqin Oasis of Northwest China. *Environmental Modelling and Software*, **24**: 1163-1170 (2009).

[3] Adhikary, P. P. and Dash, Ch. J. Comparison of deterministic and stochastic methods to predict spatial variation of groundwater depth. *Applied Water Science*, **7**: 339–348 (2014).

[4] Varouchakis, E. and Hristopulos, D. Comparison of stochastic and deterministic methods for mapping groundwater level spatial variability in

sparsely monitored basins, *Environmental monitoring and assessment*, **185**: 1–19 (2012).

[5] Shomar, B.; Fakher, S. and Yahya, A. Assessment of Groundwater Quality in the Gaza Strip, Palestine Using GIS Mapping, *Journal of Water Resource and Protection*, **2** (2): 93-104 (2010).

[6] Jie, C.; Hanting, Z.; Hui, Q.; Jianhua, W.; and Xuedi, Z. (2013, June). Selecting proper method for groundwater interpolation based on spatial correlation. In *2013 Fourth International Conference on Digital Manufacturing & Automation* (pp. 1192-1195). IEEE.

[7] Ahmad, M.; Wajid, A.; Khan, M.; Shakoor, A. and Abbas, Q. (2016). Evaluate Different interpolation techniques in GIS for Ground Water Quality Mapping, *1st National Conference on Agricultural Engineering and Sciences (NCAES2016)*, Pakistan.

[8] Caruso, C. G. and Quarta, F. Interpolation Methods Comparison, *Computers & Mathematics with Applications*, **35** (12): 109 -126 (1998).

[9] Theodossiou, N. and Latinopoulus, P. Evaluation and optimisation of groundwater observation networks using the Kriging methodology, *Environmental Modelling and Software*, **22** (7): 991-1000 (2006).

[10] Ahmadi, S. H. and Sedghamiz, A. Geostatistical Analysis of Spatial and Temporal Variations of Groundwater Level, *Environmental Monitoring and Assessment*, **129** (13): 277-294 (2007).

[11] Nikro, L.; Kompanizare, M.; Sepaskhah, A. R. and Shamshi, S. R. F. Groundwater depth and elevation interpolation by kriging methods in Mohr Basin of Fars province in Iran, *Environmental Monitoring and Assessment*, **166** (14): 387-407 (2009).

[12] Dash, J. P.; Sarangi, A. and Singh, D. K. Spatial variability of groundwater depth and quality parameters in the National Capital Territory of Delhi, *Environmental Management*, **45** (3): 640-650 (2010).

[13] Ganesh, R.; Koju, R. and Prajapati, R. R. Assessment of Groundwater Quality and Water Table Mapping of Bhaktapur Municipality, *Journal of Science and Engineering*, **5**: 43 -50 (2018).

[14] Pathak, D. Status of Groundwater Exploitation and Investigation in Terai and Inner Terai Region of Nepal, *Bulletin of Nepal Hydrogeological Association*, **3**:77-83 (2018).

[15] Khosravi, K.; Roshan, M. H. N. and Safari, A. Assessment of Geostatistical Methods for Determining Distribution Patterns of Groundwater Resources in Sari-Neka Coastal Plain, Northern Iran, *Environmental Resource Research*, **5**(2): 124-134 (2017).

[16] Mazzella, A. and Mazzella, A. The Important of the Model Choice for Experimental Semivariogram Modeling and Its Consequence in Evaluation Process, *Journal of Engineering*, **vol. 2013**, Article ID 960105, 10 Pages, (2013).

[17] Camberdella, C. A.; Moorman, T. B.; Novak, J.; Parkin, T. B.; Karlen, D.; Turco, R. and Konopka, A. R., Field Scale variability of soil properties in central Iowa Soils, *Soil Science Society of America Journal*, **58** (5): 1501-1511 (1994).

[18] Kiš, I. M. Comparison of Ordinary and Universal Kriging interpolation techniques on a depth variable (a case of linear spatial trend), case study of the Šandrovac Field. *Rudarsko Geolosko Naftni Zbornik*, **31**: 41-58 (2016).

[19] Pasini, M.; Lucio, A. and Cargnelutti Filho, A. Semivariogram models for estimating fig fly population density throughout the year, *Pesquisa Agropecuaria Brasilieira*, **49**: 493-505 (2014).

[20] Deutch, C. V. and Journal, A. G., Geostatistical software library and user's guide, New York**,** **119**: 147 (1992)

[21] Arslan, H. Estimation of spatial Distribution of groundwater level and risky areas of seawater intrusion on the coastal region in CarAYamba Plain, Turkey, using different interpolation methods. *Environmental Monitoring and Assessmen*t, **186 (**8): 5123-5134 (2014).

[22] Ahmadi, S. H. and Sedghamiz, A. Application and Evaluation of Kriging and Cokriging Methods on Groundwater Depth Mapping, *Environmental Monitoring and Assessment*, **138** (13): 357-368 (2008).